THE JOURNAL OF PHYSICAL CHEMISTRY Letters

Letter

pubs.acs.org/JPCL

Resolution of the Band Gap Prediction Problem for Materials Design

Jason M. Crowley, Jamil Tahir-Kheli, and William A. Goddard, III*

Materials and Process Simulation Center, MC139-74, California Institute of Technology, Pasadena, California 91125, United States

Supporting Information

ABSTRACT: An important property with any new material is the band gap. Standard density functional theory methods grossly underestimate band gaps. This is known as the band gap problem. Here, we show that the hybrid B3PW91 density functional returns band gaps with a mean absolute deviation (MAD) from experiment of 0.22 eV over 64 insulators with gaps spanning a factor of 500 from 0.014 to 7 eV. The MAD is 0.28 eV over 70 compounds with gaps up to 14.2 eV, with a mean error of −0.03 eV. To benchmark the quality of the hybrid method, we compared the hybrid method to the rigorous GW many-body perturbation theory method. Surprisingly, the MAD for B3PW91 is about 1.5 times smaller than the MAD for GW. Furthermore, B3PW91 is 3−4 orders of magnitude faster computationally. Hence, B3PW91 is a practical tool for predicting band gaps of materials before they are synthesized and represents a solution to the band gap prediction problem.

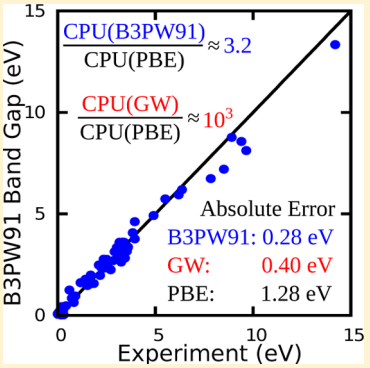

As we enter the Materials Genome Initiative (MGI) era of designing optimal materials in silico, it is essential to quickly and accurately predict the band gaps of proposed new materials. Similarly, experimentalists would benefit from an efficient computational tool for predicting band gaps prior to synthesis. We consider the problem of predicting physical band gaps to be solved by a computational method that delivers an accurate band gap for compounds spanning the whole periodic table and is simultaneously practical to compute.

Standard density functional theory (DFT) methods, such as the Perdew−Burke−Ernzerhof (PBE)[1] functional, have been the workhorse of computational materials science for decades. PBE is used by both theorists and experimentalists because of its computational speed and widespread availability in commercial codes. Unfortunately, it contains unphysical self-Coulomb repulsion,[2] leading to a systematic underestimate of band gaps.[3−5]

It is well-known that including exact Hartree−Fock exchange substantially reduces the Coulomb self-repulsion error.[6] The Heyd−Scuseria−Ernzerhof functional (HSE06) includes short-range exact Hartree−Fock exchange and has become a standard in the community.[7]

In 2012, Moussa et al.[8] and Lucero et al.[9] benchmarked HSE06 against a set of 33 compounds consisting solely of simple binary materials of the form AB. This set neglects many classes of materials such as alkali halides, transition-metal oxides (Mott insulators), transition-metal halides, systems with strong spin−orbit coupling (particularly bismuth- and lead-containing compounds), transition-metal chalcogenides, magnetic systems, and two-dimensional systems. Moussa et al. found a mean absolute deviation (MAD) of 0.32 eV with a mean error (ME) of −0.24 eV, while Lucero et al. found a MAD of 0.33 eV and a ME of −0.26 eV for this limited set of compounds.

In Moussa et al.,[8] the HSE calculations were done without spin−orbit coupling for experimental crystal structures and were compared to experimental band gaps with the spin−orbit coupling removed. For these compounds, the spin−orbit splitting is seen at the valence band maximum at the Γ point (wave vector k = 0). In these cases, the spin−orbit coupling originates from the anions (Sb, Se, Te, As). At the Γ point, the valence band consists of anion p orbitals. Spin−orbit coupling splits these triply degenerate p states at Γ into a 4-fold degenerate (j = 3/2) band and a 2-fold degenerate (j = 1/2) band. The j = 3/2 state is split upward in energy by (1/3)Δ, and the j = 1/2 state is split downward by (2/3)Δ, where Δ is the energy difference between the j = 3/2 and j = 1/2 state. For comparison to nonspin−orbit coupling HSE calculations, the known experimental band gaps of the compounds with the above anions must be increased by (1/3)Δ. For the As, Se, Sb, and Te compounds in this set, Δ is approximately 0.3, 0.4, 0.7, and 0.9 eV, respectively.

Inexplicably, Moussa et al. include the spin−orbit correction for CdTe (1.61 eV experiment corrected to 1.92 eV) but fail to include the spin−orbit correction for BAs, AlAs, AlSb, GaAs, GaSb, InAs, InSb, ZnSe, ZnTe, CdSe, MgSe, MgTe, BaSe, and BaTe. In addition, Moussa et al. use an experimental band gap of 7.22 eV for MgO instead of the low-temperature value of 7.9 eV.[9,10] These numbers appear to have been transcribed from Heyd et al.[11] When we correct these values, the MAD increases to 0.39 eV, and the mean error becomes −0.36 eV.

In Lucero et al.,[9] the MgO experimental value was corrected. These authors optimized the geometry and quoted band gaps at the optimized structures. Thus, we cannot directly compare these results to those of Moussa et al.[8] While no spin−orbit corrections were made to the experimental band gaps, it is

Received: December 24, 2015
Accepted: March 4, 2016
Published: March 4, 2016

DOI: 10.1021/acs.jpclett.5b02870
J. Phys. Chem. Lett. 2016, 7, 1198−1203

unclear from the paper whether these calculations include spin−orbit coupling or not. However, in Figure 4, the authors show their band structure for AlSb, and there is no splitting of the valence band at the Γ point. This figure suggests spin−orbit coupling may not have been included in these calculations.

The two authoritative HSE06 studies discussed above did not include the Mott insulators (FeO, NiO, MnO, CoO) or any compounds with band gaps above 8 eV. Thus, we expanded the HSE06 test set to include these Mott insulators and NaCl, β-cristobalite SiO_2, LiCl, α-quartz SiO_2, and LiF because these additional compounds are included in our present work. Using literature HSE06 values for these compounds,[12−15] the MAD and ME for Moussa et al. rise to 0.57 eV and −0.51 eV, respectively. The MAD and ME for Lucero et al. rise to 0.52 eV and −0.43 eV, respectively. These numbers are slight underestimates because we were unable to locate a literature HSE06 band gap for β-cristobalite. Thus, we assumed HSE06 obtained perfect agreement to experiment for this compound. As we show below, the MAD and ME for many-body perturbation theory (GW method) are better than these HSE06 numbers. Thus, we do not consider HSE06 any further.

The rigorous approach to solving the band gap problem is to calculate the Green's function using many-body perturbation theory (referred to as the GW method[16]). In this method, the quasiparticle excitation spectrum is calculated rigorously, whereas DFT calculates Kohn−Sham eigenvalues that are not rigorously physical. However, full GW calculations are far too computationally expensive for routine use. A nonself-consistent GW approximation, G_0W_0, has been used to improve standard DFT results for decades.[12,17−20] Recently, iterative "post-G_0W_0" methods have been used to improve G_0W_0 results.[21−25] As the next term in the expansion of the true Green's function, post-G_0W_0 should systematically improve quasiparticle energies and band gaps, albeit at a considerably higher computational cost. Despite intense effort in recent years, all GW methods are too computationally expensive for applications such as MGI.

Here, we show that the B3PW91 hybrid density functional is more accurate than GW by approximately a factor of 1.5 and is also 3−4 orders of magnitude faster computationally. Because speed and accuracy are competing properties, it is highly unusual to discover a method that dramatically improves both. This observation constitutes the main result of the Letter and suggests that B3PW91 should replace PBE as the default computational approach.

Hybrid density functionals include a fraction of exact Hartree−Fock exchange, which dramatically reduces the self-Coulomb error in DFT. Previously, we have shown that hybrid DFT matches the best G_0W_0 bulk band structure for the useful thermoelectrics and topological insulators Bi_2Te_3 and Bi_2Se_3, whereas standard DFT does not.[26] Moreover, with hybrid DFT, we performed calculations of large slabs that are inaccessible to GW. Other studies[6,8,9,27−30] of small sets of compounds have also hinted at the usefulness of hybrid functionals for solids.

To determine the quality of the B3PW91 functional (referred to as B3PW hereafter), we computed band gaps of 70 insulating compounds with band gaps ranging from 0.014 to 14.2 eV. These compounds span the entire periodic table (except for lanthanides, actinides, and solid noble gases) and include thermoelectrics, topological insulators, transition-metal oxides, photovoltaics, elemental and binary semiconductors, and transition-metal halides. To have the most accurate comparison to experiment, spin−orbit coupling was included.

No lanthanides or actinides were studied because they have strong spin−orbit coupling and partially filled 4f and 5f shells. The CRYSTAL98 source code we modified to include spin−orbit coupling does not include f orbitals. Solid noble gases were excluded because the anion is unbound, and in the solid phases, the conduction band is above the vacuum energy.[31] We know of no other study that spans as many classes of materials. Of these 70 compounds, we found GW published literature results for only 53, and there was no single study of all 53 of these compounds. The largest study[24] we found had 16 compounds. We did not perform any GW calculations. Tables S1−S3 contain references to every GW data point used in this Letter.

All of our band gap results are shown in Figure 1. Panels a, b, and c in Figure 1 plot the B3PW, GW, and PBE band gaps up to 7 eV, respectively. Figure 1d plots the band gaps for all three methods from 7 to 15 eV. The experimental band gap range is split into 0−7 and 7−15 eV for clarity only. Figures S9, S10, and S11 show all band gap results for B3PW, GW, and PBE, respectively, over the full range of 0−15 eV. All of the compounds are listed in Figures 2 and 3. The results in Figure 1a,b are for 64 out of the total 70 compounds. The results in Figure 1c for GW are for 47 out of the 53 total compounds. The mean absolute deviation (MAD) for B3PW is 0.22 eV. The MAD over all GW methods (G_0W_0 and post-G_0W_0) is 0.36 eV. The MADs for G_0W_0 and post-G_0W_0 are equal to 0.36 and 0.35 eV, respectively. The MAD for PBE is 1.10 eV. The B3PW

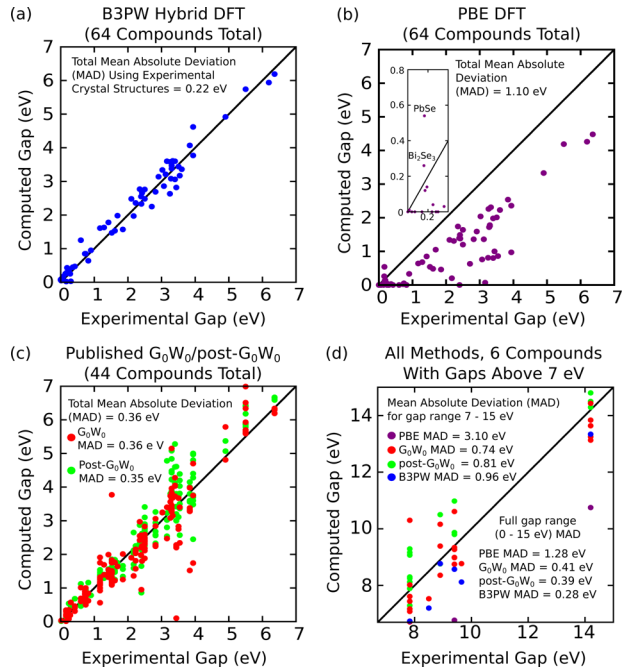

Figure 1. Calculated B3PW (hybrid DFT), GW (many-body perturbation), and PBE (standard DFT) band gaps versus low-temperature experiment. A list of the compounds studied may be found in Figures 2 and 3 and Tables S1−S3. (a) B3PW, (b) PBE, (c) GW results (G_0W_0 and post-G_0W_0) versus experiment for compounds with experimental band gaps from 0 to 7 eV. (d) B3PW, PBE, and GW data for 6 compounds with experimental band gaps larger than 7 eV. For the full band gap range, the MADs are 1.28, 0.41, 0.39, and 0.28 eV for PBE, G_0W_0, post-G_0W_0, and B3PW, respectively. Overall, the error for B3PW is 1.4 times smaller than that for post-G_0W_0. The computational cost of B3PW is 3.2 ± 2.4 times that of PBE.

DOI: 10.1021/acs.jpclett.5b02870
J. Phys. Chem. Lett. 2016, 7, 1198−1203

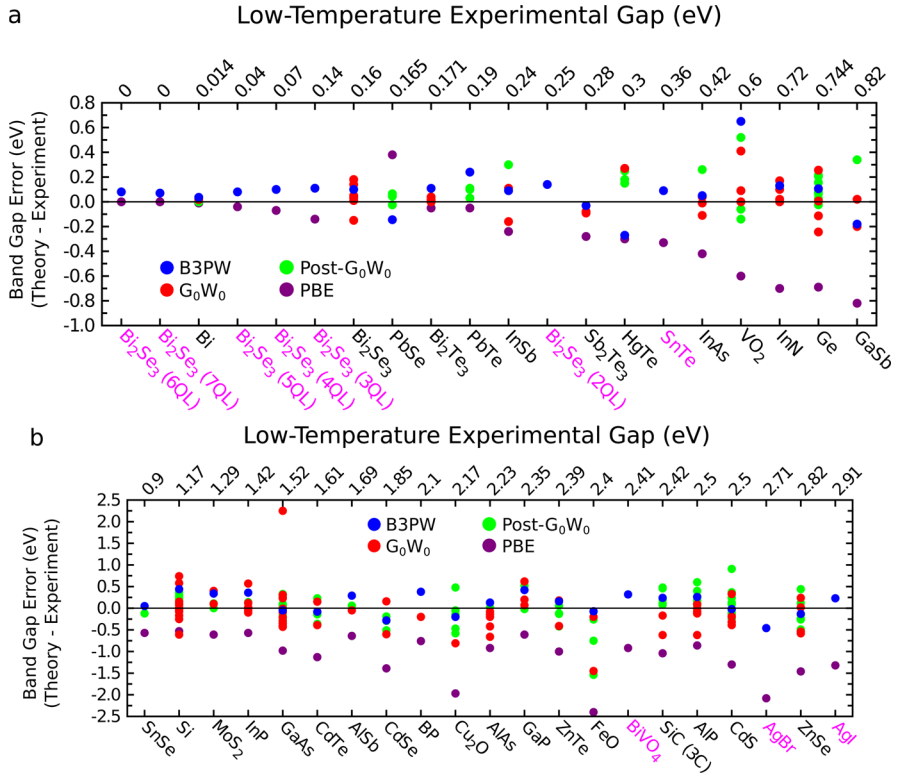

Figure 2. Difference between computed and experimental band gaps for 41 of the 70 compounds studied in Figure 1. The compounds are ordered by increasing experimental band gaps. Results are for compounds with experimental gaps from (a) 0.0 to 0.82 eV and (b) 0.9 to 2.91 eV. The horizontal lines at zero represent perfect agreement between theory and experiment. Points above these lines indicate theory has overestimated the gap, and points below these lines indicate theory has underestimated the gap. Compound names are listed on the bottom *x*-axes; experimental band gaps (low-temperature or $T \approx 0$ K when available; see Table S4 for a discussion of experimental gaps) are listed on the top *x*-axes. Compound labels in magenta are those for which our literature search found no GW results. Our B3PW results are shown by blue circles, and our PBE results are shown by purple circles. Red and green circles represent literature G_0W_0 and post-G_0W_0 results, respectively. Bi_2Se_3(NQL) refers to a two-dimensional slab of Bi_2Se_3 composed of N quintuple layers (QLs) (see ref 26 for further details). Tables S1−S3 contain all of our B3PW and PBE results, the lowest and highest GW band gap for each system, and all references from which GW results were taken.

MAD is 1.6 times smaller than the GW MAD and 5 times smaller than the PBE MAD. As is well-known,[3] PBE systematically underestimates band gaps. In fact, for 10 compounds, PBE predicts a metal (zero band gap) rather than an insulator (nonzero band gap). We found two exceptions (PbSe and Bi_2Se_3), shown in the inset to Figure 1c. These compounds have strong spin−orbit coupling and will be discussed later in the Letter.

Figure 1d shows B3PW (blue circles), PBE (purple circles), G_0W_0 (red circles), and post-G_0W_0 (green circles) results for six compounds with experimental band gaps above 7 eV. The MAD for each method over these compounds is shown in the upper left corner. The bottom right of the figure shows the MADs for the full band gap range (0−15 eV). The MADs are worse in the 7−15 eV band gap range for all methods compared to the 0−7 eV range. For the entire 0−15 eV band gap range, post-G_0W_0 is slightly better than G_0W_0. The MAD for B3PW is worse than all GW methods in the 7−15 eV range. Over the full 0−15 eV band gap range, B3PW has the lowest MAD.

To further test B3PW against the GW method, we broke down the GW data into four subsets: G_0W_0 with any starting wave function, G_0W_0 specifically using local density approximation (LDA) as the starting wave function, G_0W_0 using PBE as the starting wave function, and post-G_0W_0 (Figures S1−S8). In all four cases, B3PW had the lower MAD.

Because the only difference between our B3PW and PBE calculations is the functional, we can make a machine-independent comparison of computational cost. We find that the computational cost of B3PW is 3.2 ± 2.4 times that of PBE. It is important to note that hybrid functionals are typically $\sim 10^3$ times slower than PBE in plane-wave basis set codes. Because we used localized Gaussian basis sets, B3PW became competitive with PBE. In practical terms, this additional cost is negligible compared to the nearly 5-fold improvement in accuracy.

Plane-wave basis sets are simpler than Gaussian basis sets because they are characterized by one number: the wave vector cutoff. Gaussian basis sets require Gaussian exponents and contraction coefficients for each basis function, and different Gaussian basis sets have different numbers of basis functions. Thus, the choice of the correct Gaussian basis set is more complicated. Fortunately, computational chemists have developed highly optimized Gaussian basis sets for every element. However, these highly optimized basis sets developed for computational chemistry usually cannot be used for solids without some modification. This is because the extremely diffuse basis functions commonly used in high-quality Gaussian basis sets can lead to basis set linear dependence when used in a periodic system.[32]

Linear independence can usually be ensured by modifying the basis set so that the most diffuse Gaussian has an exponent of 0.1, as discussed in ref 30. Although minimizing the energy

DOI: 10.1021/acs.jpclett.5b02870
J. Phys. Chem. Lett. 2016, 7, 1198−1203

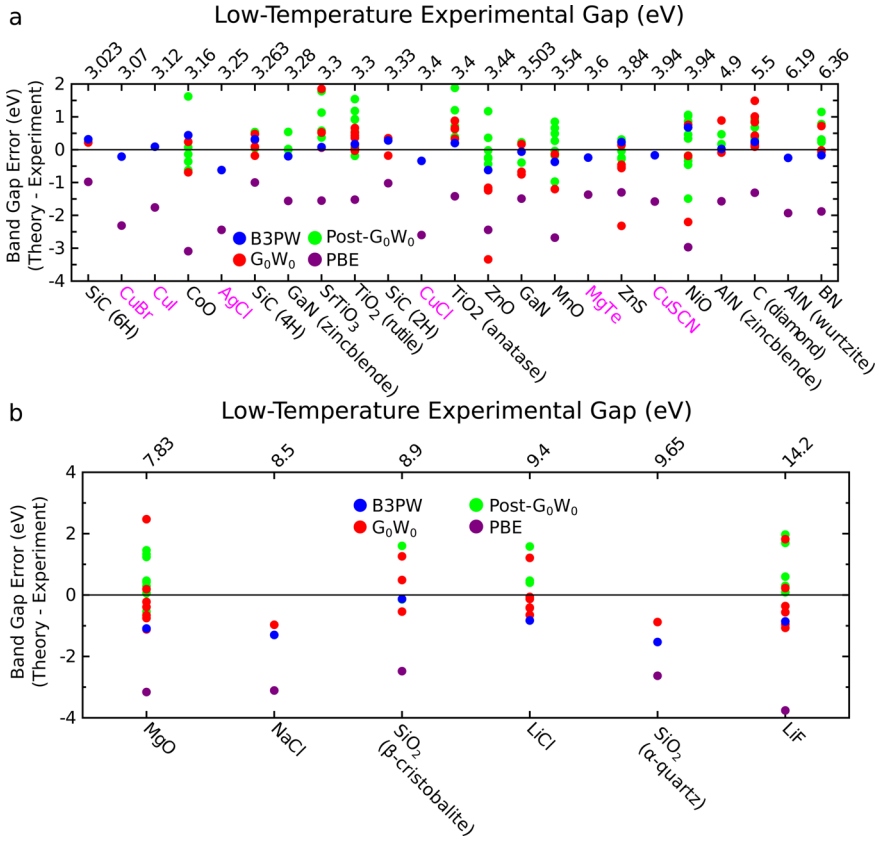

Figure 3. Same as Figure 2 for the remaining 29 compounds from Figure 1. Results for compounds with experimental gaps from (a) 3.023 to 6.36 eV and (b) 7.83 to 14.2 eV.

with respect to other Gaussian exponents can improve band gap predictions, we intentionally chose not to perform this step to keep our evaluation of B3PW as straightforward as possible. Basis sets were not tuned to a particular system and hence can be transferred to other compounds.

The basis sets used in this Letter were chosen according to a systematic recipe which is described in complete detail in section 1 of the Supporting Information. Additionally, the basis sets used in our input decks (included in the Supporting Information) are linearly independent. As a result, we believe these basis sets can be used as a template for rapid calculation of systems not considered here.

An issue for both Gaussian and plane-wave basis set calculations is whether to optimize the crystal structure or use the experimental crystal structure. A perfect theory would predict zero force for experimental structures, rendering this question irrelevant. However, DFT (regardless of basis set) tends to overestimate lattice constants by a few percent. We did our calculations at the experimental crystal structure because it is a harsher test to demand that a theory predict the correct electronic structure given only the physical structure of a material.

We now return to the inset of Figure 1b showing that PBE overestimated the band gaps for PbSe and Bi_2Se_3. These are the only two compounds where PBE overestimated the band gap. In general, spin−orbit coupling decreases the band gap by breaking the spin degeneracy. However, if the PBE band gap without spin−orbit coupling is smaller than the magnitude of the spin−orbit splitting, unphysical band repulsions may occur. Hence, for strong spin−orbit compounds with small gaps, PBE may overestimate the band gap.

Figures 2 and 3 show the band gap error broken down by compound for all 70 compounds with experimental band gaps in the 0−14.2 eV range. The compounds are ordered on the x-axis by increasing experimental band gap, and compounds with magenta labels are those where we did not find GW data. The largest B3PW band gap error occurred for α-quartz. As discussed above, these errors could be reduced by basis set optimizations. The mean signed error of B3PW is −0.03 eV.

In some cases (e.g., CoO), there is more than one measured experimental band gap. Our methodology for choosing a number for comparison is discussed in Table S4. We did not choose the experimental results closest to the B3PW prediction. Doing so would lower the overall MAD from 0.28 to 0.25 eV. On the other hand, choosing the experimental band gaps furthest from the B3PW prediction raises the MAD by 0.03 to 0.31 eV, which is less than the post-G_0W_0 MAD of 0.39 eV. Thus, we believe that B3PW solves the band gap problem.

In summary, we believe hybrid DFT can successfully resolve the band gap prediction problem for practical materials design. Standard DFT methods such as PBE have sufficient computational speed but suffer from very poor accuracy. In particular, we found the PBE functional to have a mean absolute deviation from experiment (MAD) of 1.28 eV over a class of 70 insulating compounds. While many-body perturbation methods (GW) are significantly more accurate than PBE (MAD = 0.40 eV), they are 3−4 orders of magnitude slower. Here, we have shown that the B3PW91 hybrid density functional has the best of both worlds. The MAD of B3PW91 was 0.28 eV. When used with localized Gaussian basis sets, the computational cost of B3PW91 is only 3.2 ± 2.4 times that of PBE. This remarkable result was achieved without optimization of any computational

DOI: 10.1021/acs.jpclett.5b02870
J. Phys. Chem. Lett. 2016, 7, 1198−1203

parameter, including crystal structure. Hence, B3PW91 can be employed "off the shelf" by nonexpert users to deliver excellent predictions of band gaps for materials that have not yet been synthesized.

COMPUTATIONAL METHODS

The GW data we used for comparison consisted of 387 calculations from 42 publications dating from 1987 to 2015. Of these 42 publications, 23 were from 2010 or later. Tables S1–S3 contain all references to the GW data, all references to experimental band gaps, and hyperlinks to the input decks for all of our hybrid DFT calculations. In this Letter, we study only band gaps because GW is primarily benchmarked against band gaps. We chose low-temperature experimental band gaps from ref 10 for comparison whenever possible. Table S4 details our choice of experimental band gaps.

In this work, we use the first proposed hybrid functional, B3PW91,[33] based on its prior success with topological isulators,[26] binary semiconductors,[30] and band offsets.[34] We refer to the B3PW91 functional as B3PW for simplicity. This functional was developed by Becke using the adiabatic connection.[33] B3PW makes three corrections to the LDA exchange correlation energy. First, a fraction a_0 of the LDA exchange is replaced by Hartree–Fock exact exchange. Second, Becke's 1988 gradient correction[35] for exchange is included, weighted by the parameter a_x. Finally, the Perdew–Wang 1991 (PW91) gradient correction[36] for correlation is included, weighted by the parameter a_c. These parameters were determined by a least-squares fit to 56 atomization energies, 42 ionization potentials, 8 proton affinities, and 10 total atomic energies.[33] This fitting gave $a_0 = 0.20$, $a_x = 0.72$, and $a_c = 0.81$. Becke's parametrization made no use of band gaps or any property of a solid, and we made no adjustment to these parameters.

Computing exact Hartree–Fock exchange is about 3 orders of magnitude faster with localized Gaussian basis sets[26] compared to plane-wave basis sets. Hence, we use the CRYSTAL[32] code for all of our calculations. CRYSTAL does not include spin–orbit coupling. For the cases with strong spin–orbit coupling, we used our modified version of CRYSTAL98.[26] When used for solids, the Gaussian basis sets commonly used and optimized for molecules can lead to linear dependencies. Hence, modifications for diffuse orbitals are required to remove these linear dependencies, as described in the CRYSTAL manual.[32] We also used Stuttgart pseudopotentials.[37,38] The basis set and pseudopotential (if used) for all of our calculations can be seen in the input decks included in the Supporting Information. Our systematic basis set recipe is described in full detail in section 1 of the Supporting Information. It is known that optimization of basis sets and geometries improves band gaps.[30] However, we chose not to optimize basis sets and to use experimental crystal structures because these optimizations are impractical for high-throughput applications such as MGI.

In addition to the choice of basis set, it is important to have enough irreducible k-points to obtain a fully converged result. We chose on average 103 irreducible k-points in our calculations. This number is far larger than necessary, but our calculations are so computationally inexpensive that this overkill is irrelevant. High-throughput screening becomes more practical when one can ensure convergence with a default k-point sampling. In fact, we believe our basis sets and input decks (in the Supporting Information) can be used as a template for studies on new materials.

ASSOCIATED CONTENT

Supporting Information

The Supporting Information is available free of charge on the ACS Publications website at DOI: 10.1021/acs.jpclett.5b02870.

Our recipe for basis set choice, detailed comparisons of B3PW to different levels of GW, all computed band gaps, our choices of experimental band gaps, all references for experimental geometries and band gaps, and CRYSTAL input decks for every calculation performed in this Letter (PDF)

AUTHOR INFORMATION

Corresponding Author

*E-mail: wag@wag.caltech.edu.

Notes

The authors declare no competing financial interest.

ACKNOWLEDGMENTS

We thank NSF (DMREF-1436985) and JCAP (Joint Center of Artificial Photosynthesis, DOE DE-SC0004993) for partial support. We thank Giulia Galli, Yuan Ping, and Peter A. Schultz for useful comments. We also thank Hai Xiao, Richard P. Muller, and Carver A. Mead for fruitful discussions.

REFERENCES

(1) Perdew, J. P.; Burke, K.; Ernzerhof, M. Generalized Gradient Approximation Made Simple. *Phys. Rev. Lett.* **1996**, *77*, 3865–3868.
(2) Perdew, J. P.; Zunger, A. Self-Interaction Correction to Density-Functional Approximations for Many-Electron Systems. *Phys. Rev. B: Condens. Matter Mater. Phys.* **1981**, *23*, 5048–5079.
(3) Perdew, J. P.; Levy, M. Physical Content of the Exact Kohn-Sham Orbital Energies: Band Gaps and Derivative Discontinuities. *Phys. Rev. Lett.* **1983**, *51*, 1884–1887.
(4) Sham, L. J.; Schlüter, M. Density-Functional Theory of the Energy Gap. *Phys. Rev. Lett.* **1983**, *51*, 1888–1891.
(5) Mori-Sánchez, P.; Cohen, A. J.; Yang, W. Localization and Delocalization Errors in Density Functional Theory and Implications for Band-Gap Prediction. *Phys. Rev. Lett.* **2008**, *100*, 146401.
(6) Perry, J. K.; Tahir-Kheli, J.; Goddard, W. A. Antiferromagnetic Band Structure of La_2CuO_4: Becke-3-Lee-Yang-Parr Calculations. *Phys. Rev. B: Condens. Matter Mater. Phys.* **2001**, *63*, 144510.
(7) Krukau, A. V.; Vydrov, O. A.; Izmaylov, A. F.; Scuseria, G. E. Influence of the Exchange Screening Parameter on the Performance of Screened Hybrid Functionals. *J. Chem. Phys.* **2006**, *125*, 224106.
(8) Moussa, J. E.; Schultz, P. A.; Chelikowsky, J. R. Analysis of the Heyd-Scuseria-Ernzerhof Density Functional Parameter Space. *J. Chem. Phys.* **2012**, *136*, 204117.
(9) Lucero, M. J.; Henderson, T. M.; Scuseria, G. E. Improved Semiconductor Lattice Parameters and Band Gaps from a Middle-Range Screened Hybrid Exchange functional. *J. Phys.: Condens. Matter* **2012**, *24*, 145504.
(10) Madelung, O. *Semiconductors: Data Handbook*, 3rd ed.; Springer, New York, 2004.
(11) Heyd, J.; Peralta, J. E.; Scuseria, G. E.; Martin, R. L. Energy Band Gaps and Lattice Parameters Evaluated with the Heyd-Scuseria-Ernzerhof Screened Hybrid functional. *J. Chem. Phys.* **2005**, *123*, 174101.
(12) Rödl, C.; Fuchs, F.; Furthmüller, J.; Bechstedt, F. Quasiparticle Band Structures of the Antiferromagnetic Transition-Metal Oxides MnO, FeO, CoO, and NiO. *Phys. Rev. B: Condens. Matter Mater. Phys.* **2009**, *79*, 235114.

DOI: 10.1021/acs.jpclett.5b02870
J. Phys. Chem. Lett. 2016, 7, 1198–1203

(13) Marques, M. A. L.; Vidal, J.; Oliveira, M. J. T.; Reining, L.; Botti, S. Density-Based Mixing Parameter for Hybrid Functionals. *Phys. Rev. B: Condens. Matter Mater. Phys.* **2011**, *83*, 035119.
(14) Chen, W.; Pasquarello, A. Correspondence of Defect Energy Levels in Hybrid Density Functional Theory and Many-Body Perturbation Theory. *Phys. Rev. B: Condens. Matter Mater. Phys.* **2013**, *88*, 115104.
(15) Chen, W.; Pasquarello, A. Band-Edge Levels in Semiconductors and Insulators: Hybrid Density Functional Theory Versus Many-Body Perturbation Theory. *Phys. Rev. B: Condens. Matter Mater. Phys.* **2012**, *86*, 035134.
(16) Hybertsen, M. S.; Louie, S. G. Electron Correlation in Semiconductors and Insulators: Band Gaps and Quasiparticle Energies. *Phys. Rev. B: Condens. Matter Mater. Phys.* **1986**, *34*, 5390−5413.
(17) Godby, R. W.; Schlüter, M.; Sham, L. J. Quasiparticle Energies in GaAs and AlAs. *Phys. Rev. B: Condens. Matter Mater. Phys.* **1987**, *35*, 4170−4171.
(18) Zhu, X.; Louie, S. G. Quasiparticle Band Structure of Thirteen Semiconductors and Insulators. *Phys. Rev. B: Condens. Matter Mater. Phys.* **1991**, *43*, 14142−14156.
(19) Shirley, E. L.; Zhu, X.; Louie, S. G. Core Polarization in Solids: Formulation and Application to Semiconductors. *Phys. Rev. B: Condens. Matter Mater. Phys.* **1997**, *56*, 6648−6661.
(20) Friedrich, C.; Blügel, S.; Schindlmayr, A. Efficient Implementation of the *GW* Approximation within the All-Electron FLAPW Method. *Phys. Rev. B: Condens. Matter Mater. Phys.* **2010**, *81*, 125102.
(21) Faleev, S. V.; van Schilfgaarde, M.; Kotani, T. All-Electron Self-Consistent *GW* Approximation: Application to Si, MnO, and NiO. *Phys. Rev. Lett.* **2004**, *93*, 126406.
(22) Chantis, A. N.; van Schilfgaarde, M.; Kotani, T. *Ab Initio* Prediction of Conduction Band Spin Splitting in Zinc Blende Semiconductors. *Phys. Rev. Lett.* **2006**, *96*, 086405.
(23) Shishkin, M.; Marsman, M.; Kresse, G. Accurate Quasiparticle Spectra from Self-Consistent *GW* Calculations with Vertex Corrections. *Phys. Rev. Lett.* **2007**, *99*, 246403.
(24) Chen, W.; Pasquarello, A. Band-Edge Positions in *GW*: Effects of Starting Point and Self-Consistency. *Phys. Rev. B: Condens. Matter Mater. Phys.* **2014**, *90*, 165133.
(25) Aguilera, I.; Friedrich, C.; Blügel, S. Electronic Phase Transitions of Bismuth under Strain from Relativistic Self-Consistent *GW* calculations. *Phys. Rev. B: Condens. Matter Mater. Phys.* **2015**, *91*, 125129.
(26) Crowley, J. M.; Tahir-Kheli, J.; Goddard, W. A., III Accurate Ab Initio Quantum Mechanics Simulations of Bi_2Se_3 and Bi_2Te_3 Topological Insulator Surfaces. *J. Phys. Chem. Lett.* **2015**, *6*, 3792−3796.
(27) Muscat, J.; Wander, A.; Harrison, N. On the Prediction of Band Gaps from Hybrid Functional Theory. *Chem. Phys. Lett.* **2001**, *342*, 397−401.
(28) Peralta, J. E.; Heyd, J.; Scuseria, G. E.; Martin, R. L. Spin-Orbit Splittings and Energy Band Gaps Calculated with the Heyd-Scuseria-Ernzerhof Screened Hybrid Functional. *Phys. Rev. B: Condens. Matter Mater. Phys.* **2006**, *74*, 073101.
(29) Matsuda, Y.; Tahir-Kheli, J.; Goddard, W. A., III Definitive Band Gaps for Single-Wall Carbon Nanotubes. *J. Phys. Chem. Lett.* **2010**, *1*, 2946−2950.
(30) Xiao, H.; Tahir-Kheli, J.; Goddard, W. A. Accurate Band Gaps for Semiconductors from Density Functional Theory. *J. Phys. Chem. Lett.* **2011**, *2*, 212−217.
(31) Schwentner, N.; Himpsel, F. J.; Saile, V.; Skibowski, M.; Steinmann, W.; Koch, E. E. Photoemission from Rare-Gas Solids: Electron Energy Distributions from the Valence Bands. *Phys. Rev. Lett.* **1975**, *34*, 528−531.
(32) Dovesi, R.; Saunders, V.; Roetti, C.; Orlando, R.; Zicovich-Wilson, C.; Pascale, F.; Civalleri, B.; Doll, K.; Harrison, N.; Bush, I. et al. *CRYSTAL14 User's Manual*; University of Torino: Torino, 2014.
(33) Becke, A. D. Density Functional Thermochemistry. III. The Role of Exact Exchange. *J. Chem. Phys.* **1993**, *98*, 5648−5652.
(34) Xiao, H.; Goddard, W. A. Predicted Roles of Defects on Band Offsets and Energetics at CIGS ($Cu(In,Ga)Se_2/CdS$) Solar Cell Interfaces and Implications for Improving Performance. *J. Chem. Phys.* **2014**, *141*, 094701.
(35) Becke, A. D. Density-Functional Exchange-Energy Approximation with Correct Asymptotic Behavior. *Phys. Rev. A: At., Mol., Opt. Phys.* **1988**, *38*, 3098−3100.
(36) Perdew, J. P.; Chevary, J. A.; Vosko, S. H.; Jackson, K. A.; Pederson, M. R.; Singh, D. J.; Fiolhais, C. Atoms, Molecules, Solids, and Surfaces: Applications of the Generalized Gradient Approximation for Exchange and Correlation. *Phys. Rev. B: Condens. Matter Mater. Phys.* **1992**, *46*, 6671−6687.
(37) Peterson, K. A.; Figgen, D.; Goll, E.; Stoll, H.; Dolg, M. Systematically Convergent Basis Sets with Relativistic Pseudopotentials. II. Small-Core Pseudopotentials and Correlation Consistent Basis Sets for the Post-d Group 16−18 Elements. *J. Chem. Phys.* **2003**, *119*, 11113−11123.
(38) Stoll, H.; Metz, B.; Dolg, M. Relativistic Energy-Consistent Pseudopotentials−Recent Developments. *J. Comput. Chem.* **2002**, *23*, 767−778.

DOI: 10.1021/acs.jpclett.5b02870
J. Phys. Chem. Lett. 2016, 7, 1198−1203